Indian Journal of Chemistry
Vol. 63, January 2024, pp. 65-71
DOI: 10.56042/ijc.v63i1.3936

Compatibility of benzimidazole and benzothiazole derivatives towards poly-A.poly-T DNA

Souvik Sur*[a] & Uzma Khan[b]

[a] Research and Development Center, Teerthanker Mahaveer University, Moradabad, Uttar Pradesh 244 001, India

[b] Department of Chemistry, Faculty of Engineering, Teerthanker Mahaveer University, Moradabad, Uttar Pradesh 244 001, India

E-mail: drsouvik.engineering@tmu.ac.in

Received 12 July 2023; accepted (revised) 18 December 2023

Benzimidazole (BNIMZ) and benzothiazole (BNTZA) based compounds are studied to understand their binding features with poly-A.poly-T DNA sequence and their mode of binding is also explored. According to thermal denaturation data, BNTZA slightly favors DNA stability with a 2.9°C advantage over BNIMZ. The DNA conformational stability of the B-DNA form was recorded with and without ligands by circular dichroism. The estimated docking scores support the findings from the UV denaturation investigation, and we observed that BNTZA had a higher docking score than BNIMZ. With the help of 50 ns MD simulations, additional conformational analyses have been performed. Both compounds effectively bind to the minor-grooves of AT-rich DNA sequence with a favorable binding free energy in accordance with the RMSD analysis, and pucker distribution of deoxyribose sugars. Future oligonucleotide therapies may be benefited because of the current discovery.

Keywords: Benzimidazole, Benzothiazole, AT-rich DNA, Thermal denaturation, Molecular Docking, Molecular Dynamics simulation

In chemotherapeutics, specific DNA recognition by small molecules is gaining importance day by day[1-3]. Pyrroles, imidazoles, polyamides, polybenzamides, furans, diamidines, carbazoles and pyrroloindoles are such kind of small compounds targeting specific DNA sequences in human genome[4,5]. Due to their typically crescent shaped for optimal isohelicity those molecules can fit to the major or minor grooves of DNA. The structural studies of these small molecules can open a strategic therapeutic tool to control gene expression in cells by controlling DNA sequence recognition[6].

Hurley reported in literature regarding many anticancer drugs that target DNA[7]. Anti-tumour antibiotics tend to be more specific in their interactions with DNA. Since no previous study was reported with the DNA recognition of these compounds, we have eager to know the possibilities of those drugs with DNA. Hoechst and other minor groove ligands specifically bind to AT/GC specific sequences[8-10], where Hoechst is basically benzimidazole based molecule. The hexadecamers $d(GCGCGCGCGCGCGC)_2$ and $d(ATATATATATATAT)_2$ sequences are very prone whether the chosen drugs effectively bind to DNA strands or not. Singh *et al.* earlier described the finding using the sequences[11]. Pandey *et al.* earlier described the substituent specific bisbenzimidazole binding towards AT-rich DNA[12]. Therefore, systematic studies by designing analogues with improved sequence selectivity would facilitate a comprehensive understanding of drug–DNA interaction leading to the development of better drug designing. In the present study, DNA sequence (poly-A.poly-T) recognition capabilities of two heterocyclic molecules BNIMZ and BNTZA (Fig. 1) which are basically based on benzimidazole/benzothiazole moiety with different techniques like thermal denaturation, circular dichroism, molecular docking and further molecular dynamics is studied. Since the chosen compounds are based on benzimidazole and benzothiazole; the oligonucleotide recognitions of these drugs can be an interesting finding.

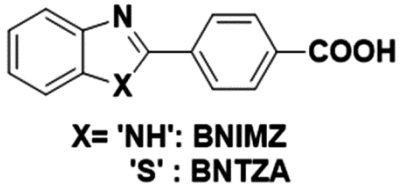

Fig. 1 — Chemical Structures of BNIMZ and BNTZA

Besides, we have compared the specific DNA (poly-A.poly-T DNA) recognition properties of two compounds. Here we have also correlated the experimental results obtained from thermal denaturation and circular dichroism study with theoretical calculations obtained from molecular docking study, MD simulations. The findings from our study can open a window for designing new minor groove binders. This information may be of use in guiding to the design of future effective DNA-binding molecules.

Results and Discussion

Thermal denaturation study by UV spectroscopy

The normal S-shaped temperature dependency of DNA's hyperchromic coefficient indicates that heating causes the helix-to-coil structural transition, which is represented in the hyperchromic appearance (Fig. 2). By comparing the DNA melting curve with and without both compounds, we observed T_m= 61.5°C for poly-A.poly-T DNA sequence and with 1:1 BNIMZ to DNA was found around 65.4°C whereas with BNTZA, it was found to be 68.3°C. The increment in the melting temperature (ΔT_m) clearly shows the enhance stability of the DNA duplex upon compound binding.

Conformational study by Circular Dichroism upon Ligand binding

Circular dichroism is a technique that can be used to quantify the DNA conformation that is most frequently seen. The sequentially heterogeneous DNA's long wavelength CD spectrum is conservative. The base pairs in the B-form are parallel to the double-helix axis, giving the molecule just a weak chirality, resulting in the relatively low peak intensities. At fixed (1:1) concentrations of BNIMZ or BNTZA in working buffer at pH=7, the positive and negative bands provide a stunning CD spectrum when (A+T) content is taken into account. Micromolar ligand concentrations cause the poly-A.poly-T DNA sequence to appear in the B-form (Fig. 3). The emergence of a spectrum with a prominent positive band at 280 nm and a weak negative band at 240 nm in the presence of ligands shows the signature curves of DNA. The signature curves of poly-A.poly-T DNA sequence resemble B-DNA form with and without ligands. So, we can conclude that no such structural changes occurred upon binding of BNIMZ as well as BNTZA with DNA. Here, we did not consider the induced CD signals obtained in each case.

Molecular Docking with DNA sequence

We have performed all the experiments using the target designed DNA sequence: poly-A_{15}.poly-T_{15}. The initial molecular docking score obtained from the most effective poses are tabulated in Table 1. The interactive nucleotides found in poly-A_{15}.poly-T_{15} DNA sequence with both the cases of with BNIMZ as well as BNTZA found in the major groove. With poly-A_{15}.poly-T_{15} DNA duplex, the substitution at N2 (here phenyl ring with –COOH group in *para* position) of benzimidazole and benzothiazole moieties favors the binding in the major groove of DNA here. The non-availability of lone-pair at N1 in case of BNIMZ, beside N2 substitution clearly disfavors the binding possibility of BNIMZ as compared to BNTZA. The availability of two lone-pairs of electrons on 'sulphur' at 1-position increases

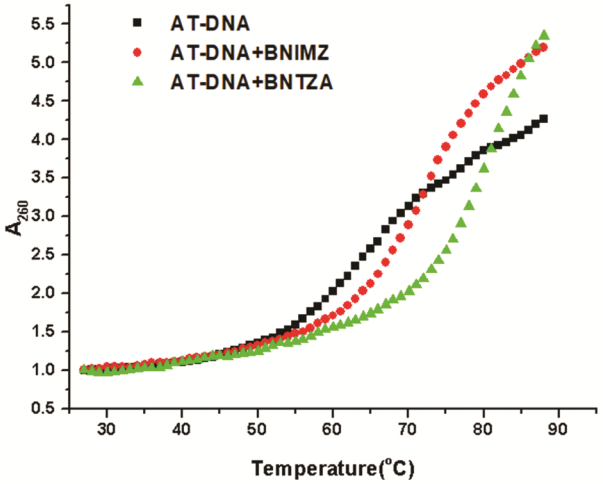

Fig. 2 — Thermal denaturation study of DNA systems with and without ligands

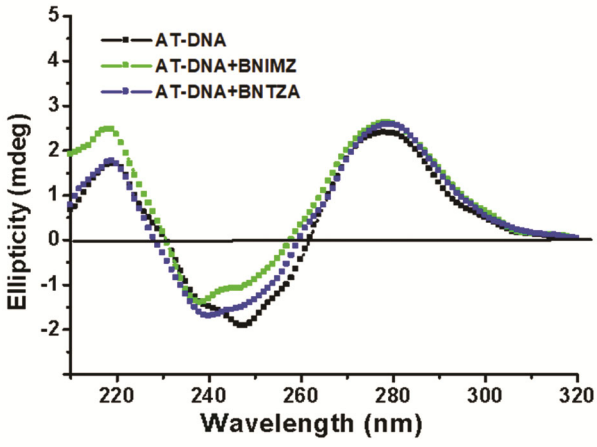

Fig. 3 — CD signature curves of DNA systems with and without ligands

Table 1 — Docking data with interactive nucleosides

Ligand	Docking pose	Docking Score with interactive residues* in DNA
BNIMZ	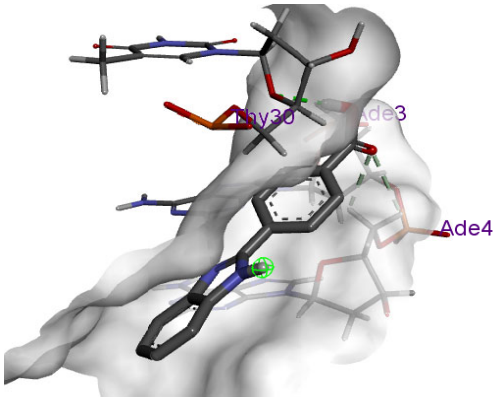	Docking Score: -5.86 Residues: A3, A4, T30
BNTZA	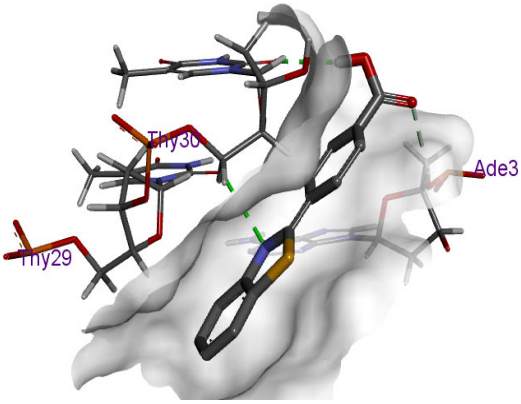	Docking Score: -6.27 Residues: A3, T29, T30

*A/Ade=Adenine, T/Thy=Thymine; Scores were obtained as binding free energies in kcal mol^{-1}

the binding interaction with neighbor nucleotides of the groove. All the found residues are tabulated in Table 1. The corresponding docking scores reflect their binding scenario in each DNA-ligand complex. As discussed, the docking score found in case of BNIZM is –5.86 which is lower than that calculated in case of BNTZA as –6.27.

Molecular Dynamics of Drug-DNA complexes

The MD simulation analysis of both docked DNA complexes with poly-A_{15}.poly-T_{15} DNA sequences were successfully done to get actual structural information as well as the stability of the complexes. Both BNIMZ as well as BNTZA complexed with DNA from the MD trajectories were performed for 50 ns. The MD averaged structures of BNIMZ as well as BNTZA with DNA sequence (Fig. 4) are found to be stable. The ligands were effectively bound with poly-A_{15}.poly-T_{15} DNA and no major deviation in structures occurred throughout the trajectories. All atom RMSD analysis showed that Drug-DNA complexes were stable throughout the simulation (Fig. 5). The double helix structures of the nucleic acid are critically based on sugar conformation. The conformation of deoxyribose (here for DNA) puckering defines the actual helical conformations of DNA by the positions of C2′ and C3′ atoms relative to a plane formed by the C1′, O4′, and C4′ atoms. The change in the duplex shape, groove widths and depths, intra-strand phosphate-phosphate distances and backbone hydration all depend on the values of puckering.

The fluctuations of ribose sugar structures throughout the MD trajectories were analyzed (Fig. 6). Not many fluctuations were found in the structure and all the final structures of the drug-DNA complexes were found to be stable with a normal B-DNA like form. Each line corresponds to the pucker pseudo-rotation angle for residues 5 to 8. Throughout the simulation, we can roughly see more population of values going from 100 to around 200 degrees which corresponds to a C2'-endo configuration present for B-DNA.

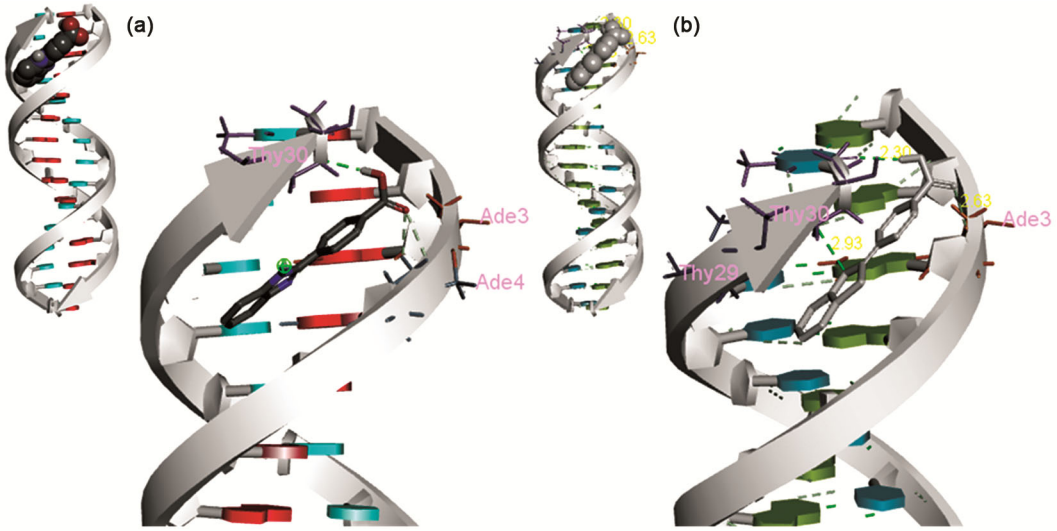

Fig. 4 — Docked structures of BNIMZ (A) and BNTZA (B) after MD simulation

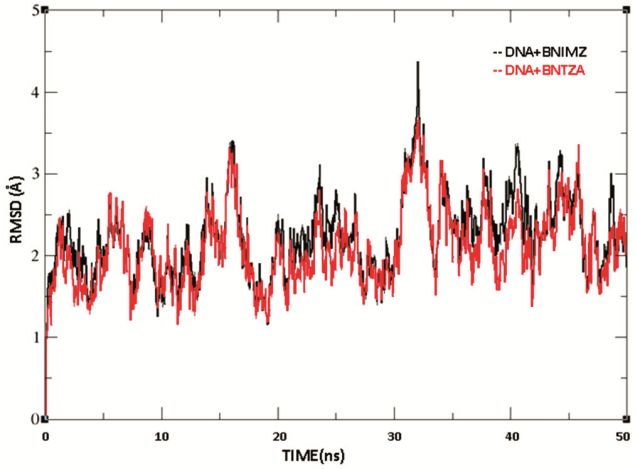

Fig. 5 — All–atom RMSD overlapping plot for BNIMZ (in black curve) and BNTZA (in red curve) docked with DNA

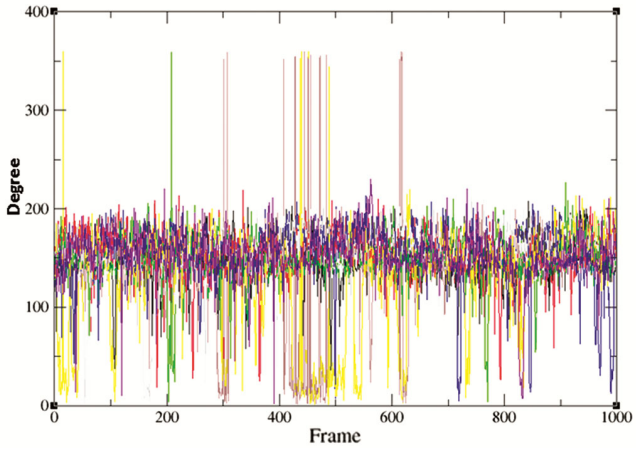

Fig. 6 — Ribose sugar fluctuations in puckering from MD trajectory analysis for residues 5 to 8 (in Black, Red, Green, Blue line)

MM/PBSA Binding Energy Calculation

The MM/PBSA programme was used to evaluate the binding energy (BE). Table 2 lists the total BEs of the drug-DNA complexes, taking into account contributions from van der Waals, electrostatic, surface-polar, and non-polar energy sources. BNTZA, which demonstrated the highest docking scores with DNA, also demonstrated a comparable pattern in the calculation of binding energy using molecular mechanics and Poison-Boltzmann surface area (MM/PBSA). The binding free energies were discovered in a manner consistent with the present study's docking score.

A significant contribution from van der Waals interactions were found to be –30.82 kcal/mol in case of BNTZA favoring the summarized binding free energy of –24.79 kcal/mol; whereas in BNIMZ, shows comparatively less binding free energy of –21.84 kcal/mol. Besides van der Waals interactions, the other thermodynamic parameters like electrostatic, surface-polar, and non-polar energy, solvation energies contribute significantly and the effective binding free energies were also contributed significantly in calculations.

Structural analysis through DNA-groove binding

As we know that in the ideal situation, there are two hydrogen bonds present between adenine and thymine and the distance between N6 - O4 is 2.8 to 3.0 Å and N1- N3 is 2.8 Å. We have calculated the number and distances of hydrogen bonds before and after MD simulation and those are tabulated in Table 3. A little fluctuation was observed in both the

Table 2 — MM/PBSA binding energy* computation of the compounds-DNA systems

Ligand	$\triangle E_{vdw}$	$\triangle E_{GB}$	$\triangle E_{surf}$	$\triangle G_{Gas}$	$\triangle G_{solv}$	$\triangle G_{Free}$
BNIMZ	–26.05 ± 3.17	6.30± 0.83	–2.09 ± 0.16	–26.05 ± 3.19	4.20± 0.73	–21.84 ± 2.68
BNTZA	–30.82 ± 2.22	8.89± 0.55	–2.86 ± 0.12	–30.82 ± 2.22	6.03± 0.58	–24.79 ± 1.97

*All the energies are calculated in kcal mol^{-1}; vdw: van der Waal, surf: surface, solv: solvation

Table 3 — Details of Hydrogen bonding between Adenine and Thymine

Base Pair	No. of H-bond	Atoms involved	*Distance (Å)		Atoms involved	*Distance (Å)	
			BNIMZ	BNTZA		BNIMZ	BNTZA
A-----T	2	N6 - O4	2.92(2.88)	2.95(2.88)	N1 - N3	2.88(2.90)	2.89(2.90)
A-----T	2	N6 - O4	2.92(2.88)	2.91(2.88)	N1 - N3	2.77(2.90)	2.96(2.90)
A-----T	2	N6 - O4	2.93(2.88)	3.01(2.88)	N1 - N3	2.95(2.90)	2.90(2.90)
A-----T	2	N6 - O4	2.83(2.88)	2.79(2.88)	N1 - N3	2.94(2.90)	2.96(2.90)
A-----T	2	N6 - O4	2.86(2.88)	3.14(2.88)	N1 - N3	2.84(2.90)	2.93(2.90)
A-----T	2	N6 - O4	2.88(2.88)	3.14(2.88)	N1 - N3	3.10(2.90)	2.96(2.90)
A-----T	2	N6 - O4	3.51(2.88)	2.88(2.88)	N1 - N3	2.97(2.90)	2.89(2.90)
A-----T	2	N6 - O4	2.79(2.88)	2.91(2.88)	N1 - N3	2.99(2.90)	2.82(2.90)
A-----T	2	N6 - O4	3.01(2.88)	2.91(2.88)	N1 - N3	3.01(2.90)	2.98(2.90)
A-----T	2	N6 - O4	2.89(2.88)	2.92(2.88)	N1 - N3	3.04(2.90)	3.04(2.90)
A-----T	2	N6 - O4	2.79(2.88)	2.93(2.88)	N1 - N3	2.89(2.90)	3.08(2.90)
A-----T	2	N6 - O4	2.89 (2.88)	2.88(2.88)	N1 - N3	3.05(2.90)	2.97(2.90)
A-----T	2	N6 - O4	3.12(2.88)	2.92(2.88)	N1 - N3	2.87(2.90)	2.78(2.90)
A-----T	2	N6 - O4	2.92(2.88)	3.12(2.88)	N1 - N3	2.82(2.90)	2.90(2.90)
A-----T	2	N6 - O4	2.97(2.88)	2.75(2.88)	N1 - N3	2.88(2.90)	2.88(2.90)

*Data mentioned in the parentheses were calculated before MD

Table 4 — Analysis of DNA base-pair parameters

Parameters	Step	Shift	Slide	Rise	Tilt	Roll	Twist
Base-pair step parameters	Initial*	-0.00±0.00	-0.20±0.00	3.37±0.00	0.01±0.00	-2.81±0.00	35.89±0.00
	BNIMZ	-0.09±0.39	-0.93±0.53	3.36±0.38	-015±0.16	-0.59±0.52	33.63±2.58
	BNTZA	-0.09±0.39	-0.93±0.53	3.36±0.38	-015±0.16	-0.59±0.52	33.63±2.58
Base-pair helical parameters	Initial*	0.08±0.00	0.00±0.00	3.38±0.00	-4.54±0.00	-0.01±0.00	36.00±0.00
	BNIMZ	-1.50±0.89	-0.19±0.51	3.32±0.38	-1.08±5.74	0.09±0.08	34.15±2.70
	BNTZA	-1.07±0.23	-0.14±0.62	3.20±0.28	1.22±0.76	0.77±0.09	35.43±1.70

*Data calculated before MD

bonds present between Adenine and thymine, but the number of hydrogen bonds found remains 2. From this observation, we can conclude the rigidity of DNA duplex structure upon groove binding with both ligands BNIMZ and BNTZA.

On the other hand, the Web 3DNA 2.0 programme[13,14] was used to calculate the helical parameters for duplexes docked with BNIMZ and BNTZA. Only rise tends to an average value within 50 ns of the inter-base pair parameters shift, slide, and rise showing changes during hybridization. The A and B forms can be distinguished using this parameter. Although there was some variability in the inter-base pair parameters shift, slide, and rise (Table 4), they continued to exist in B-DNA form.

Conclusion

From the present study, we have found that BNIMZ and BNTZA bind successfully in the minor groove of poly-A_{15}.poly-T_{15} DNA sequences. Due to the three-dimensional structures both compounds and the presence of –NH as well as -S- group/atom in BNIMZ and BNTZA respectively, both compounds preferentially bind to the minor groove pockets of DNA. The interactions of nucleotides with the heterocyclic molecules and the availability of lone pairs increase the feasibility of non-covalent bonding in minor groove of DNA. Thermal denaturation study reveals that BNTZA slightly favors the stability of DNA with 2.9 °C over BNIMZ. Circular dichroism experiments showed that the DNA conformational stability of the B-DNA form of DNA while recorded

with ligands. The calculated docking scores support the observation resulting from UV denaturation study as we have found a better docking score with BNTZA over BNIMZ. Further confirmational analysis was confirmed with 50 ns MD simulations. The RMSD analysis, the pucker distribution of deoxyribose sugars and binding energy calculations supports that both compounds effectively bind to the grooves of AT-rich DNA sequence with favorable binding free energy. Present finding can open a window for designing more DNA groove binders which can help in future oligonucleotide therapeutics.

Experimental Section

Synthesis of Compounds

Both the compounds BNIMZ and BNTZA were synthesized by reported procedure[15,16]. All the synthesized compounds were further purified by column chromatography and characterized through NMR, IR, mass spectrometry The poly-A_{15}.poly-T_{15} DNA sequences were procured from Merck and the working buffer 10 mM sodium cacodylate buffer at pH=7.0 was made with standard protocol.

Thermal melting determination of DNA

The construction of thermodynamic models and the analysis of potential structural biopolymer conformations depend heavily on the thermal measurements of DNA. The present study examined the structural stability of DNA in the presence of ligands using thermal denaturation. The number of helical areas and the number of untwisted regions are identical when the temperature approaches the melting point (T_m). T_m is the temperature where 50% of a DNA sequence is in the helix shape and the remaining 50% is not. A further rise in temperature causes a significant shift in equilibrium in favor of a rise in the proportion of single strands. Increased UV absorption intensity occurs along with this process. The relationship between UV absorption intensity and temperature is shown by the melting curve. Using a UV spectrophotometer, melting curves of polynucleotides with fixed (Compound/DNA=1:1) concentrations were observed at a fixed wavelength of 260 nm, which is the wavelength at which DNA absorbs the most energy. We have used 10 mM sodium cacodylate buffer at pH=7.0 in the whole experiment.

Circular Dichroism Experiment

The Circular dichroism (CD) measurements were recorded using a Chirascan Plus CD spectrometer from Applied Photophysics. The measurements were carried out using 2 mm Suprasil quartz cells from Hellma Analytics. The spectra were recorded between 210 and 320 nm, with a bandwidth of 1 nm, time per point of 1 s, and three repetitions. The RMS noise of CD signal is around 0.03 mdeg at 250 nm.

Molecular Docking Protocol

For molecular docking experiment of both the compounds with poly-A_{15}.poly-T_{15} DNA sequence, we have chosen AutoDock which is an excellent non-commercial docking program widely used[17,18]. Further, we employed a stochastic Lamarckian genetic algorithm for docking methodology and simultaneously minimizing its scoring function with better thermodynamic stability of the ligand bound to the DNA duplexes. We have used AutoDock Vina 4.2 for docking of chosen drugs *i.e.* bendamustine, albendazole and mebendazole. Intermediary steps, such as pdbqt files for DNA and ligands preparation and grid box creation were completed using Graphical User Interface program AutoDock Tools (ADT). We have manually added the polar hydrogens, Kollman charges to the targeted DNA sequences. The initial files of targeted DNA and drugs were saved in PDBQT format. AutoGrid was used for the preparation of the grid map using a grid box and the dimensions of the grid-box was set to $45 \times 45 \times 45$ xyz points with a spacing of 0.275 Å. The docking had been done in the grid box constituting minor and major groove of DNA so that we can compare whether the drugs bind to major or minor groove. Biovia Discovery Studio was used to analyze the obtained docked structures[19,20]. The nucleotides with close contact with all three analogues were labeled and those are called as the interactive residues. All the possible interactions which are present in each of the docked complex like H-bonding or other possible van der Waal interactions were checked and analyzed.

Molecular Dynamics Study

As we have found all four drugs effectively bound to AT-rich DNA as compared to GC-sequence, we have further initiated molecular dynamics approach for getting better insight pictures of those docked DNAs. The best docked structures considered for further molecular dynamics analysis using AMBER 20 package[21,22]. Molecular dynamics simulation offers the prospect of a detailed description of the dynamic structure of ions and water at the molecular level. All the parameters were generated using literature values

using the GAUSSIAN 03 and RESP program of AMBER 20. The most effective force-field for our target AT DNA was taken as parmbsc0[23].

MD run was performed for 50 ns for each system. RMSD with "least-square fitting" on the DNA backbone atoms was calculated for DNA and the ligand's heavy atoms with PTRAJ module. The binding free energy (ΔG_{bind}) was calculated by the MM/PBSA method[24,25]. We have taken the final 5 ns trajectory from each simulation for MM/PBSA binding free energy calculation in the current study.

Structural analysis

All the structural analysis was done by Web 3DNA 2.0 web server[13,14]. Web 3DNA (w3DNA) 2.0 is a significantly enhanced version of the widely used w3DNA server for the analysis, visualization, and modeling of 3D nucleic-acid-containing structures.

Acknowledgements

SS is thankful to the facility provided by Teerthanker Mahaveer University, Moradabad, Uttar Pradesh, India and granting seed money for the completion of this project *via* ref. TMU/R.O./2020-21/Seed money /002 dated 19/06/2021. UK is thankful for getting fellowship from Teerthanker Mahaveer University, Moradabad, Uttar Pradesh, India.

References

1 Patil S D, Rhodes D G & Burgess D J, *AAPS J*, 7 (2005) E61.
2 Khanna A, *Can Res*, 75 (2015) 2133.
3 Anchordoquy T J, Allison S D, Molina M dC, Girouard L G & Carson T K, *Drug Disc Today*, 6 (2001) 463.
4 Houck C M, Rinehart F P & Schmid C W, *J Mol Bio*, 132 (1979) 289.
5 Dunham I, Hunt A R, Collins J E, Bruskiewich R, Beare D M, Clamp M & Ren Q, *Nature*, 402 (1999) 489.
6 Warren C L, Kratochvil N C, Hauschild K E, Foister S, Brezinski M L, Dervan P B & Ansari A Z, *Pro Nat Aca Sci*, 103 (2006) 867.
7 Hurley L H, *Nat Rev Can*, 2 (2002) 188.
8 Pjura P E, Grzeskowiak K & Dickerson R E, *J Mole Bio*, 197 (1987) 257.
9 Harshman K D & Dervan P B, *Nucleic Acids Research*, 13 (1985) 4825.
10 Singh M P, Joseph T, Kumar S, Bathini Y & Lown J W, *Chem Res Toxi*, 5 (1992) 597.
11 Singh M, Sur S, Rastogi G K, Jayaram B & Tandon V, *Mol Bio Sys*, 9 (2013) 2541.
12 Pandey S, Sur S & Tandon V, *J India Chem Soc*, 95 (2018) 1607.
13 Li S, Olson W K & Lu X J, *Nucleic Acids Res,* 47 (2019) W26.
14 Zheng G, Lu X J & Olson W K, *Nucleic Acids Res,* 37 (2009) W240.
15 Rbaa M, Abousalem M A S, Galai M, Lgaz H, Lakhrissi B, Warad I & Zarrouk A, *Arabian J Sci Eng*, 46 (2021) 257.
16 El-Meguid E A A & Ali M M, *Res Chem Intermed*, 42 (2016) 1521.
17 Huey R, Morris G M & Forli S, *The Scripps Research Institute Molecular Graphics Laboratory*, 10550 (2012) 1000.
18 Rizvi S M D, Shakil S & Haneef M, *EXCLI J*, 12 (2013) 831.
19 Jejurikar B L & Rohane S H, *Drug Designing in Discovery Studio*, 2021.
20 Pawar S S, & Rohane S H, *Asian J Res Chem*, 14 (2021) 1 (https://doi.org/10.5958/0974-4150.2021.00014.6).
21 Salomon-Ferrer R, Case D A & Walker R C, *Wiley Interdisciplinary Reviews: Computational Molecular Science*, 3 (2013) 198.
22 Case D A, Cheatham III TE, Darden T, Gohlke H, Luo R, Merz Jr K M & Woods R J, *J Comp Chem*, 26 (2005) 1668.
23 Pérez A, Marchán I, Svozil D, Sponer J, Cheatham T E, Laughton C A & Orozco M, *Biophy J*, 92 (2007) 3817.
24 Genheden S & Ryde U, *Expert opinion on drug discovery*, 10 (2015) 449.
25 Kuhn B, Gerber P, Schulz-Gasch T & Stahl M, *J Med Chem*, 48 (2005) 4040.